Force Discrimination of Finger Pads Using Improved Hand Haptic Interface

Haruhisa Kawasaki* and Tetsuya Mouri

Faculty of Engineering, Department of Mechanical Engineering, Gifu University, Japan

Abstract

This paper presents improvements to a developed hand haptic interface and the experimental results from a force discrimination test of finger pads. The hand haptic interface combines newly developed one-dimensional (1D) force display devices for each finger pad using the 3D fingertip Haptic Interface Robot called the HIRO III equipped with a 3D hand-pose measurement system. The force display is smaller and lighter than our previous device, and a glove was added to fix multiple force display devices to the human hand. Using the method of constant stimuli, the difference threshold of finger pads on the middle phalanx, proximal phalanx, and metacarpal head of the index finger and thumb were evaluated to obtain the basis for the optimum haptic interface design.

Keywords

Haptic interface, Force display, Multi-fingered hand, Finger pad, Force discrimination

Introduction

Haptic interfaces that present force and tactile feeling to the fingertips of human have been investigated over the last two decades [1-5]. Some of these interfaces [3-5] provide three-dimensional (3D) force feelings to the fingertips, covering the workspace of the human arm. In the real world, however, humans manipulate objects based on tactile feelings and forces on their finger pads as well as their fingertips. For example, medical doctors search for tumors during breast palpation and manipulate internal organs during surgery using both fingertips and finger pads. A hand haptic interface that displays force feeling not only at the fingertips but also at the pads is needed in order to practice such medical procedures in a virtual environment. As another example, when a humanoid robot is telecontrolled by a human operator, the hand haptic interface is useful for dexterous manipulation.

In the human finger, the nerve endings that discriminate touch sensations are densest at the fingertip, and less dense on the finger pads. Hence, the finger has higher sensitivity to 3D forces on the fingertip than on the pad [6]. Thus, a haptic interface for the hand comprised of one-dimensional (1D) finger-pad force display devices and a 3D fingertip force display device is likely to be effective for use in a virtual environment. Previously developed finger force display devices [7-10] have been

Kawasaki and Mouri. Int J Robot Eng 2018, 3:009

Kawasaki and Mouri. Int J Robot Eng 2018, 3:009

ISSN: 2631-5106 | • Page 2 of 10 •

wearable, but had only open-loop control due to limitations in the setting area of the finger pad. They were not small enough for multiple devices to be attached to a finger. Our group previously developed a hand haptic interface for use in a virtual reality environment [11,12] that consisted of 1D finger-pad force-display devices and a 3D fingertip haptic interface robot HIRO II. The hand haptic interface system was large-scale because the hand pose of the operator was measured by the combination of a 3D orientation-tracking sensor and a 3D position-tracking sensor. Furthermore, the size of the 1D finger-pad force-display device needed to be much more compact in order for plural devices to be worn on human fingers.

There have been many reports of human perception with regard to force magnitude [13,14], force direction [15-19], magnitude and direction of friction moment [20,21], edge sharpness perception [22], and multi-point force perception [23-25]. These studies, however, focused only on force perception at the fingertips. No study has evaluated the force discrimination of the finger pads. Research on the biomechanics of the finger pad is useful in the design of a finger-pad force display, but wearable finger-pad force display devices may actually reduce the force sensitivity of the human finger, because they must be firmly fixed to the finger with a belt or loop fastener in order to function properly. Therefore, reducing the size of the finger-pad force display device, and developing a wearable method for multiple finger-pad force display devices for the human hand may affect force discrimination.

This paper presents a modified hand haptic interface and experimental results from force discrimination tests of finger pads with users. The hand haptic interface combines newly developed 1D force display devices for each finger pad with the 3D fingertip haptic interface called the HIRO III

[26] equipped with a 3D hand-pose measurement system. The force display has been improved by a reduction in size, and we evaluate a glove that allows the user to easily wear multiple force display devices. The force discrimination of the finger pads was assessed to gain a basis for the development of an optimum haptic interface design. Using the method of constant stimuli [27], we evaluated the difference threshold of finger pads on the middle phalanx, proximal phalanx, and metacarpal head of human fingers using the modified force display device. Comparison with previous force display devices is presented.

Hand Haptic Interface

Design concept of the hand haptic interface

Based on knowledge [28] that the density of tactile sensory organs in the human finger is highest in the fingertips and relatively low in the finger pads and palm, a hand haptic interface that applies 3D force feelings to the finger tips and 1D force feelings to the finger pads and palm was developed from a previously reported interface [11,12]. A conceptual illustration of the design is shown in Figure 1. In the figure, the human operator is displayed receiving 3D forces at the fingertips and 1D forces in the direction normal to the surface of the finger pads and palm through the 1D force display devices. The 1D force display devices are attached to the proximal phalange and metacarpal head of the thumb and middle phalange, the proximal phalange, and the metacarpal head of the finger. The metacarpal head is on the palm. In this situation, the compactness and light weight of the finger-pad display are key features. Further knowledge of the force discrimination of the finger pads will contribute to making force display devices.

Modified hand haptic interface
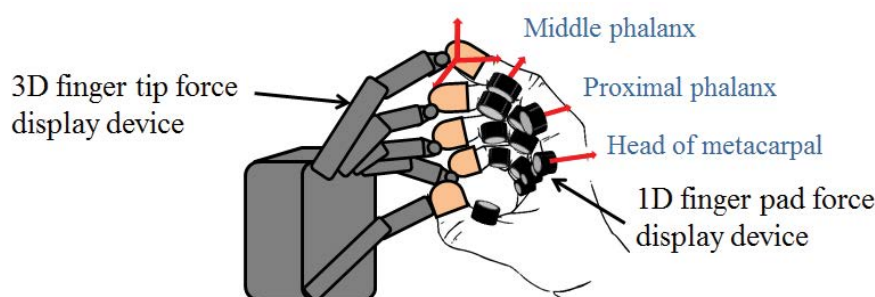
The previous hand haptic interface used the

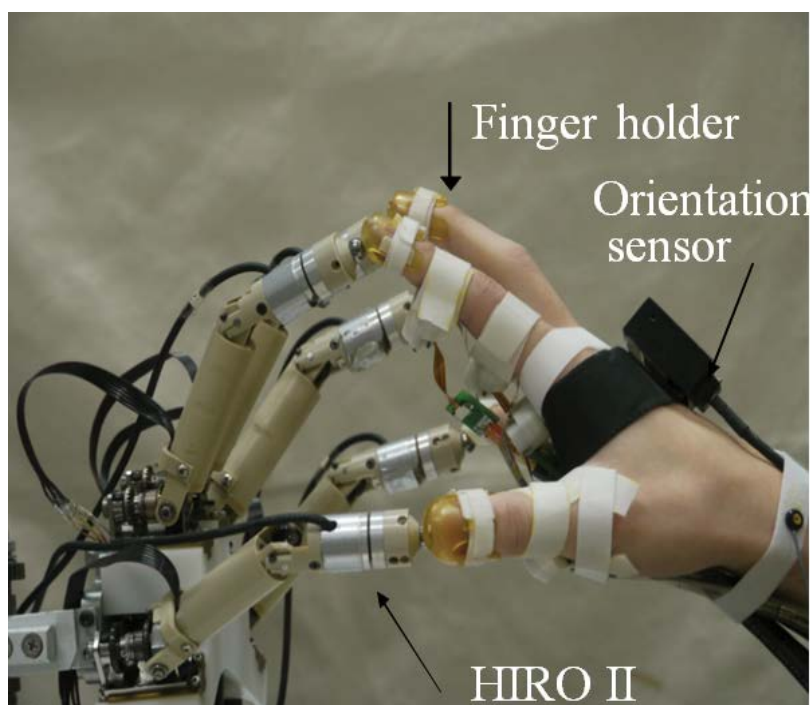**Figure 1:** Concept of proposed hand haptic interface.

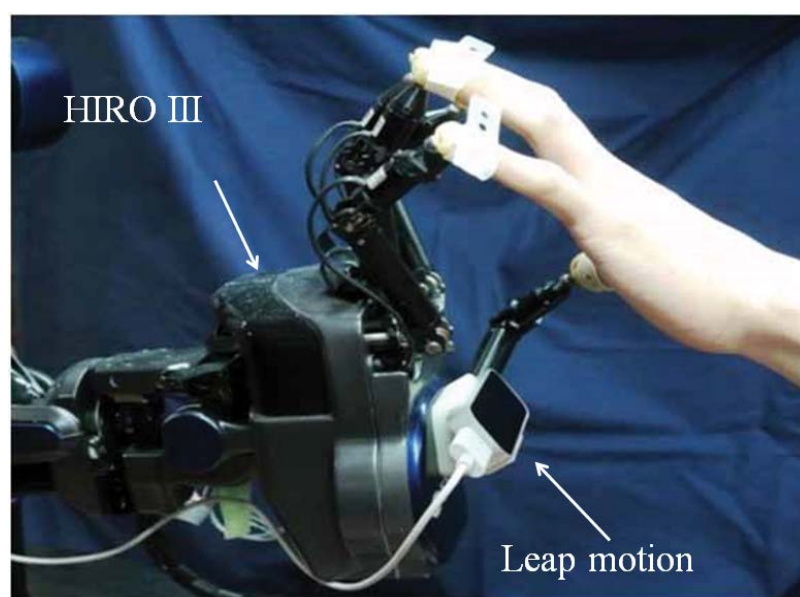**Figure 2:** Previously developed hand haptic interface.

Figure 3: Modified hand haptic interface.

HIRO II [12] as a 3D fingertip haptic interface, as shown in Figure 2. In this system, the hand pose of the operator was measured by the combination of a 3D orientation-tracking sensor (InertiaCube, InterSense, Inc.) and a 3D position-tracking sensor (Optorak Certus, Northern Digital, Inc.). The finger joint angles of the operator's hand were calculated using the inverse kinematics of the finger, based on the positions of the fingertips (measured by HIRO II), and on the position of the wrist (measured by the 3D position sensor). The approach of measurement was large in size; LED markers were sometimes dropped from the view of the 3D position-tracking sensor, and the system required computation of inverse kinematics.

To solve these issues, we developed a modified hand haptic interface based on the design concept that applied 3D fingertip forces to the previously developed multi-fingered haptic interface robot HIRO III, an updated version of HIRO II. We adopted a new hand position measurement device called Leap Motion, which was mounted on the palm of

Kawasaki and Mouri. Int J Robot Eng 2018, 3:009

ISSN: 2631-5106 | • Page 4 of 10 •

HIRO III, as shown in Figure 3. This measurement device could continually measure the operator's hand position when his/her fingertips were connected to the HIRO III. The finger joint angles of the operator's hand were measured directly. Figure 4 shows an example of a virtual reality environment in which the human fingers were displayed as a skeleton model, and fingertips and finger joints were displayed using small spheres.

The mechanisms of the HIRO III are described in detail in [26]. Briefly, the HIRO III can present force and tactile feeling at the five fingertips of the human hand. HIRO III is designed to be completely safe and is similar to the human arm, both in shape and mobility. The mechanism of the HIRO III consists of a 6 DOF arm and a 15-DOF hand, with a thumb and four fingers. Each finger has three joints, allowing 3 DOF. The first joint, relative to the base of the hand, allows abduction/adduction. The second and third joints allow flexion/extension. The thumb is similar to the fingers, except for the reduction gear ratio and the movable ranges of joints 1 and 2. To measure the finger loading, a three-axis force sensor is installed at the second link of each finger. The user must wear finger holders over his/her fingertips to manipulate the haptic interface. Each finger holder has a ball attached to a permanent magnet at the force sensor tip so as to form a passive spherical joint, which has two roles. First, ad-

justments can be made to compensate for the differences between the human finger orientation and the haptic finger orientation. Second, the operator is able to remove his/her fingers from the haptic interface in case of a malfunction. The suction force generated by the permanent magnet is 5 N.

1D Force Display Device

Configuration of force display device

The haptic device for the finger pads and palm needed to be small and lightweight so that it could be attached to the finger pads and palm. Meanwhile, the magnitude of the applied force had to be large enough to simulate reality in virtual object manipulation. The device had to be easy to wear, and could not obstruct the movement of the hand. Previously developed haptic devices for the fingertips or pads [7-10] have been problematic in that forces could not be applied simultaneously to the finger pads of the finger and palm because of size limitation, or because the applied forces from the low-torque motor were insufficient. Therefore, we developed a new 1D force display device, shown in Figure 5a, that is compact and lightweight and can be attached to the finger and palm at three points. This 1D force display device consists of a body, a hook-and-loop fastener (which is wrapped around the finger pad), and a tactile sensor.
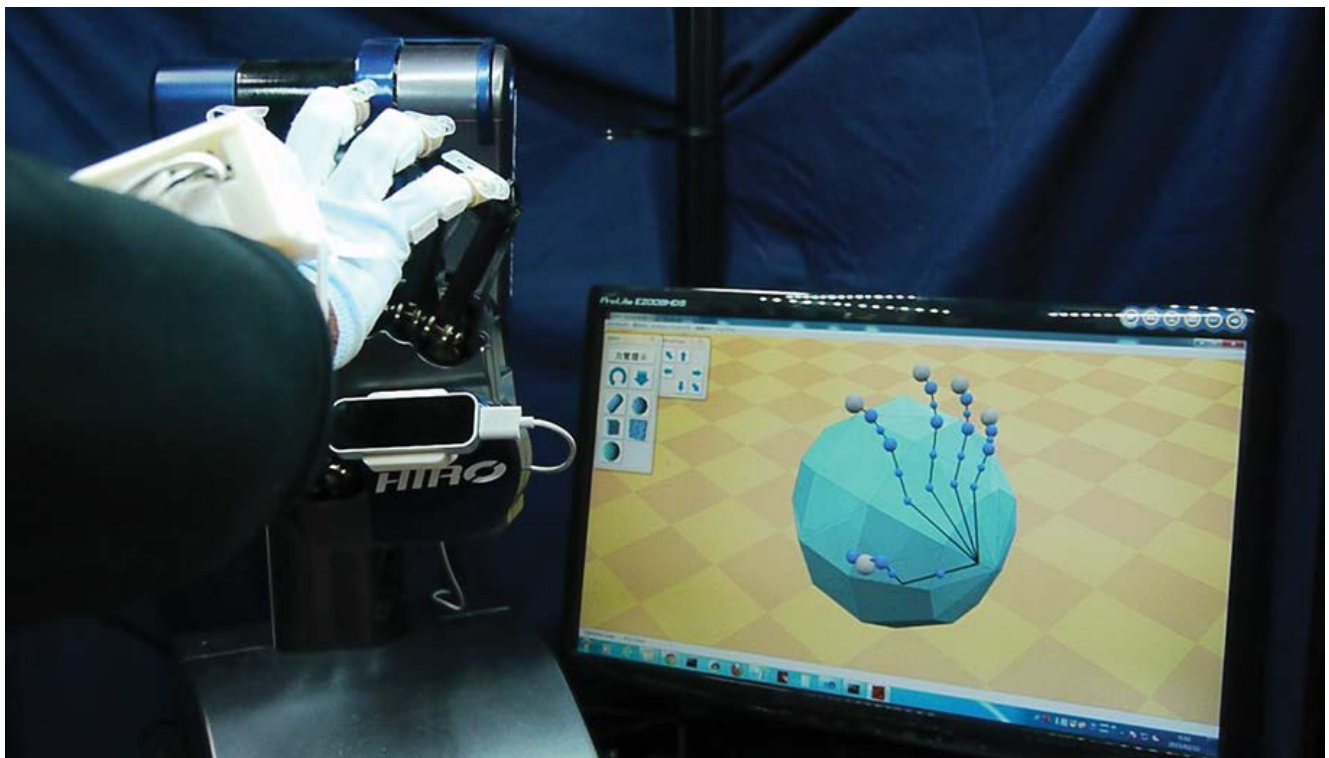

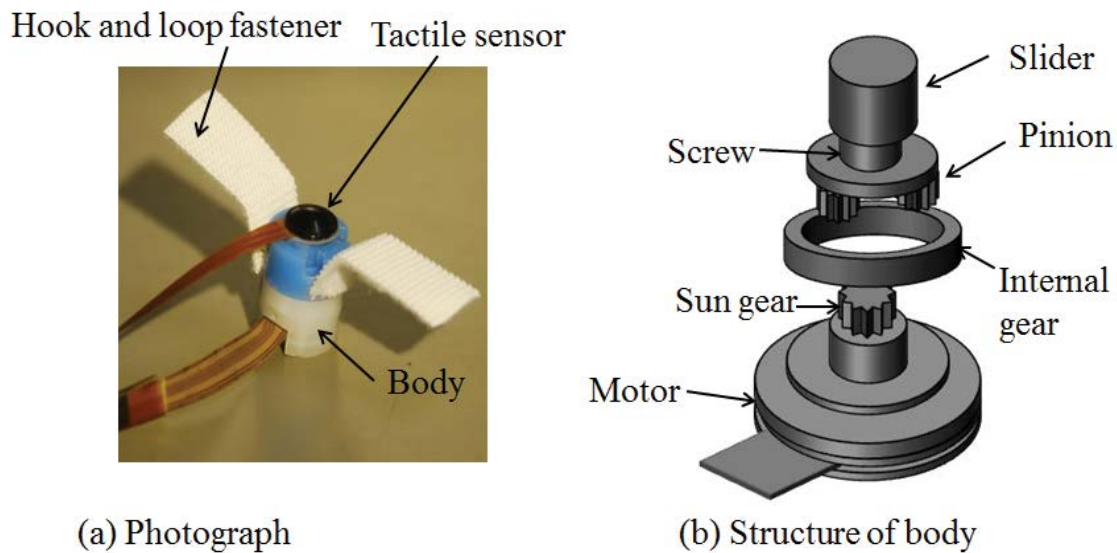**Figure 4:** Virtual reality environment.

Kawasaki and Mouri. Int J Robot Eng 2018, 3:009

ISSN: 2631-5106 | • Page 5 of 10 •

Figure 5: Newly developed finger pad force display.
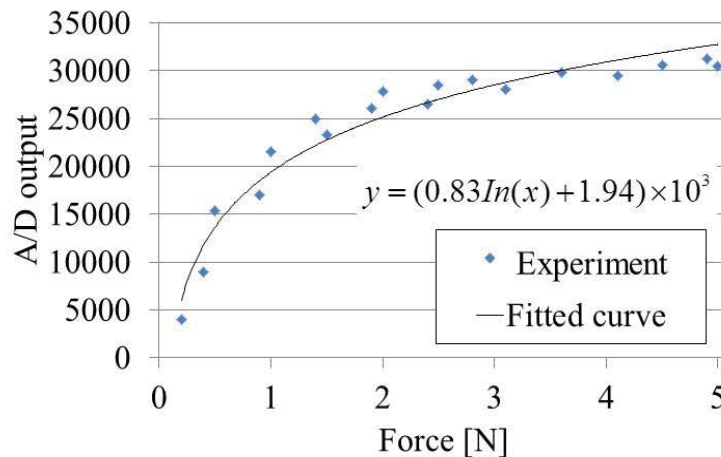

$$y = (0.83 In(x) + 1.94) \times 10^3$$

Figure 6: Relation between A/D converter output and input force to the pressure sensor.

The mechanical structure of the device is shown in Figure 5b. The finger-pad force display device is driven by a flat brushless motor equipped with a Hall sensor (EC10, Maxon Motor), and has a maximum torque of 1.76×10^{-4} Nm, a maximum rotational velocity of 2.3×10^3 rad/s, a mass of 0.81 g, and a diameter of 0.01 m. Reduction gears with a reduction ratio of 3.67 are attached to the rotor of the motor, and a screw mechanism with a pitch of 0.5 mm is attached to the output gear axis of the reduction gears. The nut of the screw mechanism that moves up and down with the rotation of the motor has a 4-mm movement range and contacts the finger pad. The mass, output force, and volume of the body are 2.9 g, 5.6 N, and 2.14×10^{-7} m³, respectively, which are 0.6, 2.1 and 0.46 times those of our previously developed 1D force display device [12]. The finger-pad force display device contains a pressure sensor (Inastomer, Inaba Rubber Co.). A relation between 16 bit AD converter and force which was added to the pressure sensor using a force gage is shown in Figure 6. The measurement data was fitted by a logarithmic curve. The contact force is measured using this curve in the closed-loop control system.

This finger-pad force display is attached to the human finger with a hook and loop fastener, as shown in Figure 7. As we had used this attachment method in a previous device [12], we knew it required a relatively long time to attach the many finger-pad force displays to the hand. To reduce this time, we tested a glove equipped with plural finger force displays, as shown in Figure 8. The fingertips of the glove were cut so that the HIRO III could be connected to the operator's fingers.

Kawasaki and Mouri. Int J Robot Eng 2018, 3:009

ISSN: 2631-5106 | • Page 6 of 10 •

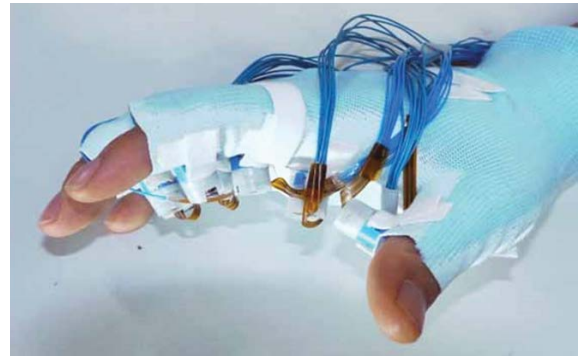**Figure 7:** Human finger fixed two finger pad force displays.

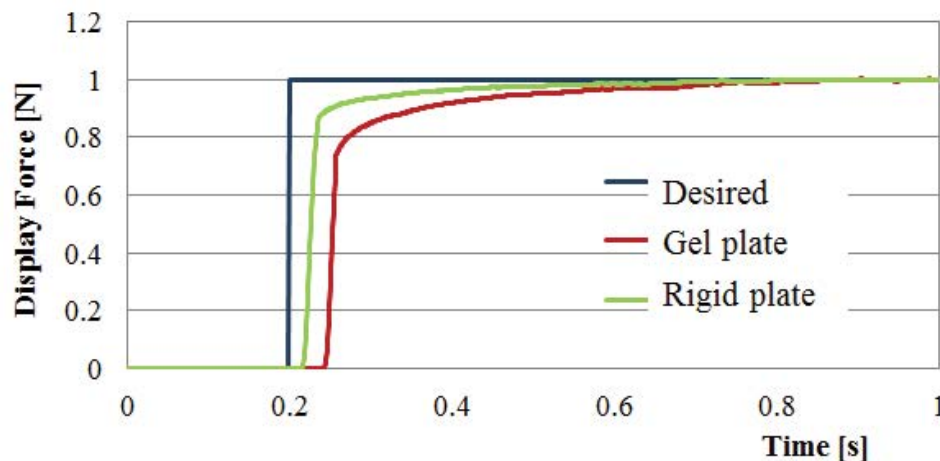**Figure 8:** Glove fixed with finger pad force displays.

Figure 9: Force responses of the finger-pad display device.

Step responses

The force responses of the finger-pad force display device were measured for a rigid plate and a gel plate, as shown in Figure 9. The gel plate [29] (Exseal Co.), which was 5-mm thick and had a hardness measure of 5 on an ASKER durometer (Type C), was wedged between the sensor and the force display device. This plate was selected because its hardness is similar to that of human skin. The desired force was a step with magnitude 1 N; The closed-loop control was a proportional-integral (PI) force feedback control; the settling time for rigid and gel plates were 142 and 300 ms, respectively, which were 0.46 and 0.89 times those of the previous version of the device. Both responses show a time delay at the start point because the motor driver checks the phase relation of motor winding at about 120 ms. The responses showed that the presented force reached the desired level for both the rigid plate and gel plate.

Experiment

Experimental setup

Human perceptions of force at the finger pads were examined using the glove by the method of constant stimuli. Subjects were 5 men, ages 21-24. Each subject was asked to turn up his palm. Five measurement points were taken: Middle phalanx, proximal phalanx, metacarpal head of the index finger, and proximal phalanx and metacarpal head of the thumb. Three levels of standard stimulus forces - 1, 2, and 3 N-were evaluated. Nine comparison stimuli, in the range of ± 0.8 N of each standard stimulus force in steps of 0.2 N, were randomly displayed. The standard stimulus was always displayed before the comparison stimulus. Both standard and comparison stimuli were displayed until the subject indicated feeling the displayed force. This experiment was executed two times for each subject.

Experimental results

Figure 10 shows the experimental results of force discrimination at the middle phalanx, proximal phalanx and metacarpal phalanx of the index finger with standard stimulus 1 and 3 N. The curve was fitted using the normal cumulative distribution function. In the case of a standard stimulus of 1 N, the point of subjective equality (PSE) of the proxi-

Kawasaki and Mouri. Int J Robot Eng 2018, 3:009

ISSN: 2631-5106 | • Page 7 of 10 •
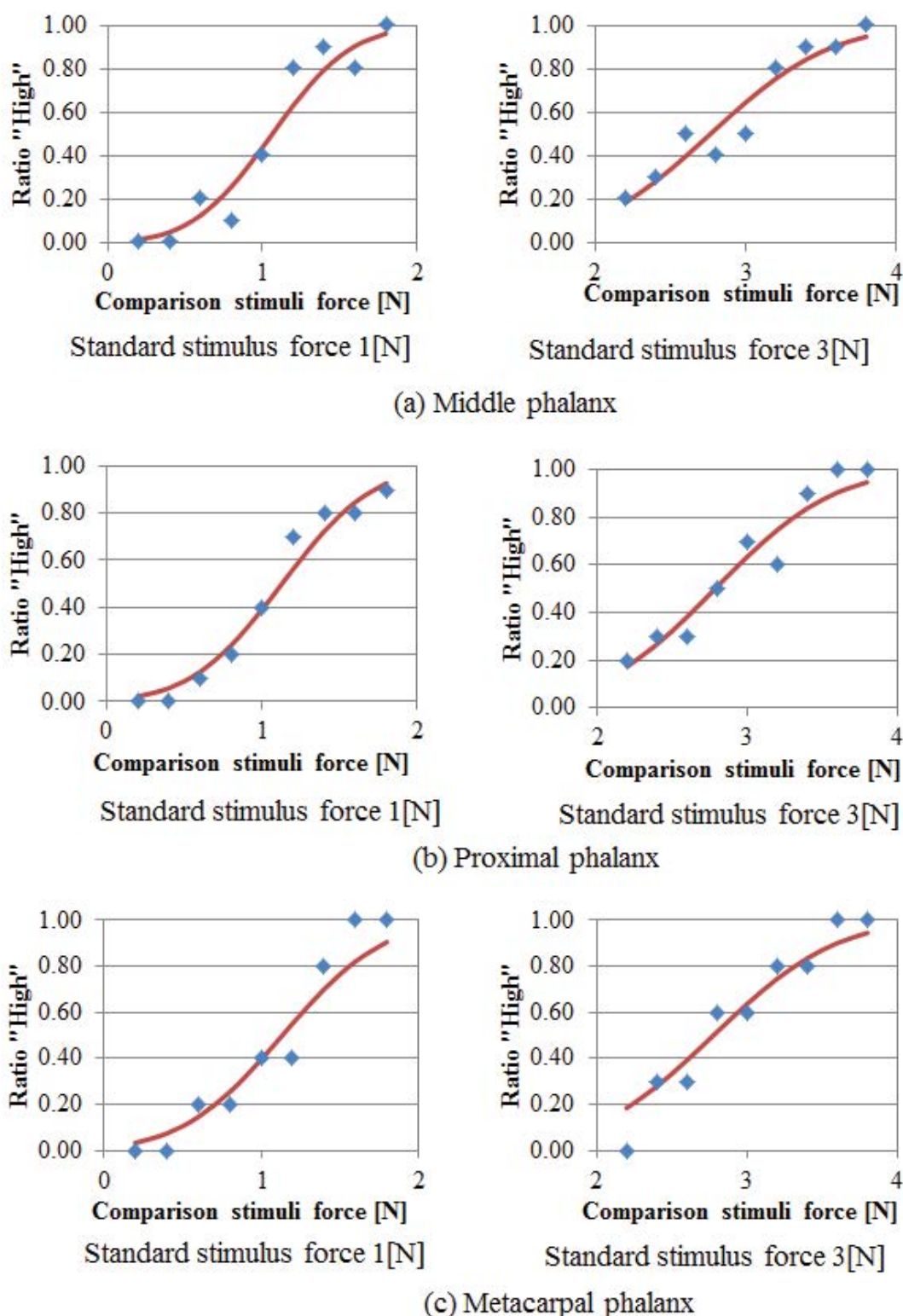
Figure 10: Force discrimination of index finger with standard stimulus 1 and 3 N.

mal phalanx was 1.1 N, and the difference threshold at the upper/lower limen of the proximal phalanx was 0.311 N.

Figure 11 shows the experiment results of force discrimination at the proximal phalanx and meta-carpal phalanx of the thumb with a standard stimulus of 1, 2 and 3 N. The curve was fitted using the normal cumulative distribution function. In the case of a standard stimulus of 1 N, the point of subjective equality (PSE) of the proximal phalanx was 1.1 N, and the difference threshold at the upper/lower
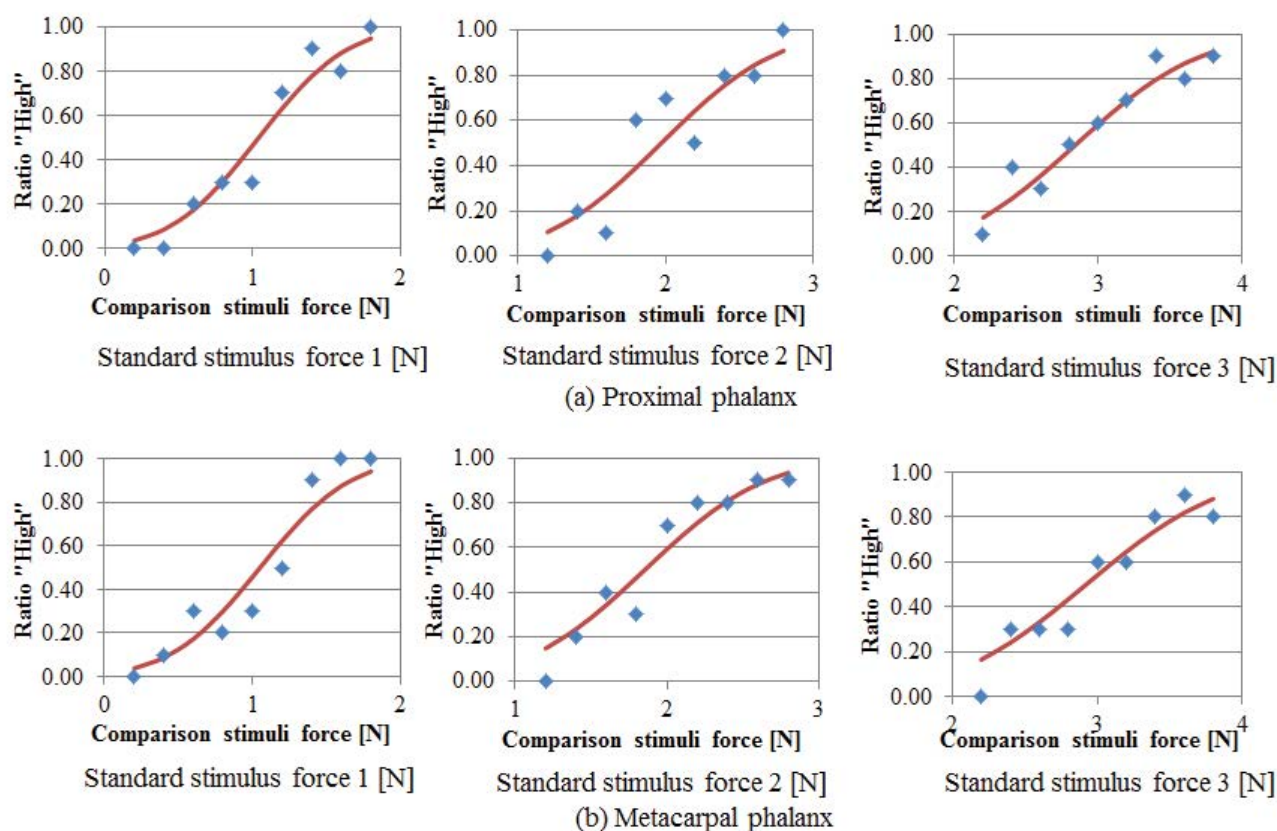
Kawasaki and Mouri. Int J Robot Eng 2018, 3:009

ISSN: 2631-5106 | • Page 8 of 10 •

Figure 11: Force discrimination of thumb with standard stimulus 1 and 2 [N].

Table 1: Difference threshold.

Standard stimulus force [N]	Thumb		Index finger		
	Proximal phalanx	Metacarpal head	Middle phalanx	Proximal phalanx	Metacarpal head
1	0.317	0.321	0.274	0.311	0.341
2	0.418	0.42	0.357	0.374	0.382
3	0.458	0.499	0.425	0.421	0.432

Table 2: Comparison of difference threshold between fixing methods of finger pad force displays at a standard stimulus force of 1 N.

Device type	Proximal phalanx	Metacarpal head	Middle phalanx	Proximal phalanx	Metacarpal head
Glove [N]	0.317	0.321	0.274	0.311	0.341
Fastener [N]	0.403	0.411	0.362	0.379	0.418

limen of the proximal phalanx was 0.317 N, which was almost the same as that of the index finger.

Experiment results of other difference thresholds are listed in Table 1. This shows that the difference thresholds of the middle phalanx, proximal phalanx and metacarpal head increased with distance from the fingertip, and that the difference threshold of the thumb was almost the same as that of the index finger.

Table 2 presents a comparison of the difference threshold between two fixing methods: The glove shown in Figure 8, and the hook and loop fastener shown in Figure 7. The standard stimulus force was 1 N. In both cases, the difference thresholds of the middle phalanx, proximal phalanx, and metacarpal head increased with distance from the fingertip. The difference threshold of the glove was about 20% less than the hook and loop fastener. We suggest that this was probably due to the weaker bind force of the glove. This means that fixing method influences difference threshold, and a weaker bind force is recommended.

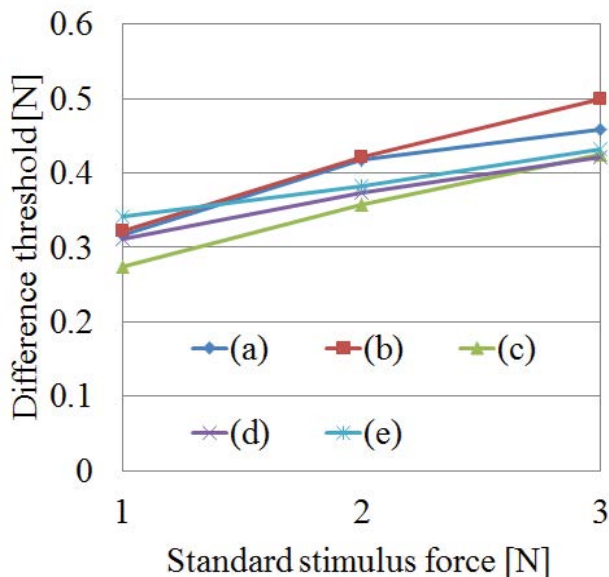Figure 12 shows the difference threshold at dif-

Figure 12: Difference threshold at three standard stimulus forces: a) Proximal phalanx of thumb; b) Metacarpal head of thumb; c) Middle phalanx of index finger; d) Proximal phalanx of index finger; and e) Metacarpal head of index finger.

Figure 13: Just noticeable difference at three standard stimulus forces: a) Proximal phalanx of thumb; b) Metacarpal head of thumb; c) Middle phalanx of index finger; d) Proximal phalanx of index finger; and e) Metacarpal head of index finger.
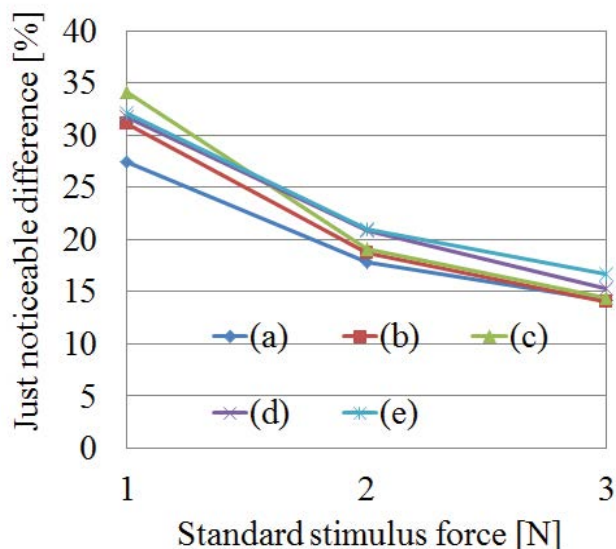
ferent standard stimulus forces. Figure 13 shows the just-noticeable difference (JND) at different standard stimulus forces. In both figures, (a) Is the proximal phalanx of thumb; (b) The metacarpal head of the thumb; (c) The middle phalanx of the index finger; (d) The proximal phalanx of the index

finger; and (e) The metacarpal head of the index finger. Figure 12 indicates that the difference threshold spreads linearly with the standard stimulus force, but Figure 13 shows that the JND decreases. These results demonstrate that the ability to perceive small forces depends on the site on the finger; in cases of large force, however, the difference in the perceptive faculty of different finger sites is relatively small.

Conclusion

This paper presented a modified hand haptic interface and its force discrimination at the finger pads. The hand haptic interface consisted of the HIRO III equipped with a 3D hand-pose measurement device and newly developed 1D finger-pad force display devices for the finger pads. The finger-pad force display was improved in size (smaller and lighter), and we used a glove to attach multiple force display devices. The force discriminations of the finger pads were evaluated using the method of constant stimuli. The perceptive faculty of force of finger pads declined with increasing distance from the fingertip, but in the case of large force, the difference between sites on the finger was relatively small. Moreover, the difference between index finger and thumb was relatively small. These results mean that there is no need to change the specifications of the finger-pad force display due to digit (finger or thumb). Comparison between glove and fastener showed that the bind force to fix the finger influenced the difference threshold, and that a weak bind force was preferable. In future, the hand haptic interface will is extended to display force feeling on the thumb and four fingers, and to evaluate its usability in virtual environments.

Acknowledgments

References

1. H Kawasaki, T Hayashi (1993) Force feedback glove for manipulation of virtual objects. Jour of Robotics and Mechatronics 5: 79-84.

2. M Bouzit, G Burdea, G Popescu, R Boian (2002) The rutgers master ii - new design force-feedback glove. IEEE/ASME Trans on Mechatronics 7: 256-263.

Kawasaki and Mouri. Int J Robot Eng 2018, 3:009

ISSN: 2631-5106 | • Page 10 of 10 •

3. Y Adachi, Takahiro Kumano, Akio Ikemoto, Asaki Hattori, Naoki Suzuki (2002) Development of a haptic device for multi fingers by Macro-Micro structure. Journal of the Robotics Society of Japan 20: 725-733.

4. H Kawasaki, T Mouri (2007) Design and control of five-fingered haptic interface opposite to human hand. IEEE Transaction on Robotics 23: 909-918.

5. I Galiana, J Brenosa, J Barrio, M Ferre (2012) New Control Architecture Based on PXI for a 3-Finger Haptic Device Applied to Virtual Manipulation. Proc of EuroHaptics 112-123.

6. SJ Lederman (1991) Skin and touch. Encyclopedia of Human Biology 7: 51-63.

7. T Grieve, Y Sun, JM Hollerbach, SA Mascaro (2009) 3-D force control on the human fingerpad using a magnetic levitation device for fingernail imaging calibration. Proc of 3rd Joint Eurohaptics Conference and Symposium on Haptic interfaces for Virtual Environment and Teleoperator System 411-416.

8. K Minamizawa, S Fukamachi, H Kajimoto, N Kawakami, S Tachi (2008) Wearable haptic display to present mass and internal dynamics of virtual objects. TVRSJ 13: 15-23.

9. T Aoki, H Mitake, S Hasegawa, M Sato (2009) Wearable haptic device to present contact sensation, based on cutaneous sensation using thin wires. TVRSJ 14: 421-428.

10. IM Koo, K Jung, JC Koo, J Nam, YK Lee (2008) Development of soft-actuator based wearable tactile display. IEEE Trans on Robotics 24: 548-558.

11. H Kawasaki, Y Doi, S Koide, T Endo, T Mouri (2010) Hand haptic interface incorporating 1D finger pad and 3d fingertip force display devices. Proc of ISIE 1869-1874.

12. H Kawasaki, S Koide, T Mouri, T Endo (2011) Development of a finger pad force display for a hand haptic interface. Virtual Reality 93-106.

13. XD Pang, HZ Tan, NI Durlach (1991) Manual discrimination of force using active finger motion. Percept Psychophys 49: 531-540.

14. HZ Tan, MA Srinivasan, B Eberman, B Cheng (1994) Human factors for the design of force-reflecting haptic interfaces. Dynamic Systems and Control 55-1: 353-359.

15. F Barbagli, K Salisbury, HZ Tan (2006) Haptic discrimination of force direction and the influence of visual information. ACM Transactions on Applied Perception 3: 125-135.

16. HZ Tan, F Barbagli, K Salisbury, C Ho, C Spence (2006) Force-direction is not influenced by reference force direction. Haptics-e 4: 1-6.

17. I Elhajj, H Weerasinghe, A Dika, R Hansen (2006) Human perception of haptic force direction. Proc of IROS 989-993.

18. E Dorjgotov, GR Bertoline, L Arns, Z Pizlo, SR Dunlop (2008) Force amplitude perception in six orthogonal directions. Symposium on Haptics Interfaces for Virtual Environment & Teleoperator Systems 121-127.

19. T Endo, T Kanno, M Kobayashi, H Kawasaki (2010) Human perception test of discontinuous force and a trial of skill transfer using a five-fingered haptic interface. Journal of Robotics 2010: 1-14.

20. H Kawasaki, Y Ohtuka, MO Alhalabi, T Mouri (2006) Haptic rendering and perception of frictional moment. Proc of EuroHaptics 201-206.

21. H Kawasaki, Y Ohtuka, T Mouri (2008) Development of haptic device to display frictional moment. Proc of IEEE SMC International Conference on Distributed Human-Machine Systems 410-415.

22. J Park, AJ Doxon, WR Provancher, DE Johnson, HZ Hong (2011) Edge sharpness perception with force and contact location information. Proc of IEEE World Haptics Conference 21-24.

23. HH King, R Donlin, B Hannaford (2010) Perceptual thresholds for single vs. multi-finger haptic interaction. Proc of IEEE Haptics Symposium 95-99.

24. LB Prorquis, M Konyo, S Tadokoro (2011) Enhancement of human force perception by multi-point tactile stimulation. Proc of IROS 3488-3493.

25. H Kawasaki, S Koide, T Endo, T Mouri (2012) Development of a hand haptic interface and its basic experimental evaluation. Proc of International Symposium on Innovations in Intelligent Systems and Applications 5.

26. T Endo, H Kawasaki, T Mouri, Y Ishigure, H Shimomura, et al. (2011) Five-fingered haptic interface robot: HIRO II. IEEE Trans on Haptics 4: 14-27.

27. DG Altman (1991) Practical statistics for medical research. Chapman and Hall/CRC.

28. RS Johanson, AB Vallbo (1979) Tactile sensibility in the human hand: relative and absolute densities of four types of mechanoreceptive units in glabrous skin. Jour of Physiol 286: 283-300.

29. WEB of Exseal Corporation.